

for RH parameterization exceeding saturation are not available. Both absolute humidity (v) and suspended haze droplet concentration (w_A) can be expressed in terms of RH variability. Absolute (v) and relative (RH) humidity are inter-related through the ambient temperature T .

Sulfates are the major RH-active ingredient of both urban and rural aerosols; so is sodium chloride for maritime species. The atmosphere is never free from HAE, with greatest concentrations near the surface and scale heights on the order of 1 km. Above RH = 90%, suspended water droplets have developed carrying the HAE essence in solutions. Average values of w_A lie between 0.01 and 1 mg/m³. The humidity parameterization in MPM is demonstrated by the examples given in Figures 12 and 13.

Pressure variability comes into play when modeling height dependencies. Cumulative calculations of α/β for a slanted radio path through the neutral atmosphere (e.g., ground-to-satellite) encounter pressures, $P = 100$ to 0 kPa, which narrows the molecular absorption lines until they vanish altogether. Pressure-, Zeeman-, and Doppler-broadening [(A-11)] have to be considered over the height range 0 to 90 km. Another need for a formulation of pressure profiles arises from spectroscopic studies applying pressure-scanning techniques. A simulation of laboratory measurements discussed in Section 2.3 is exhibited in Figure 14.

4. EXPERIMENTAL-VERSUS-MODEL (MPM) DATA

Corroborative experimental data of sufficient quality to scrutinize MPM predictions are scarce. Reliability, precision, and limited scope of supporting meteorological data often compromise the accuracy of results deduced from field observations. Generally, laboratory experiments are more accurate by simulating controlled electromagnetic and atmospheric conditions crucial to validate a specific model aspect. In this manner, contributions from water vapor lines (22 and 183 GHz) and from oxygen lines (48 to 70, 119 GHz) have been evaluated [1], [4], [10], [11], [16]. Theoretical refinements are motivated to improve the interpretation of empirical laboratory data by establishing a connection to the physics of the problem. For example, a set of our unpublished dispersion (N') results on dry air, taken during 1976 between 53.6 and 63.6 GHz, provided reference data for an elaborate reformulation of interference coefficients that describe the 60 GHz O₂ bandshape [10]. The new

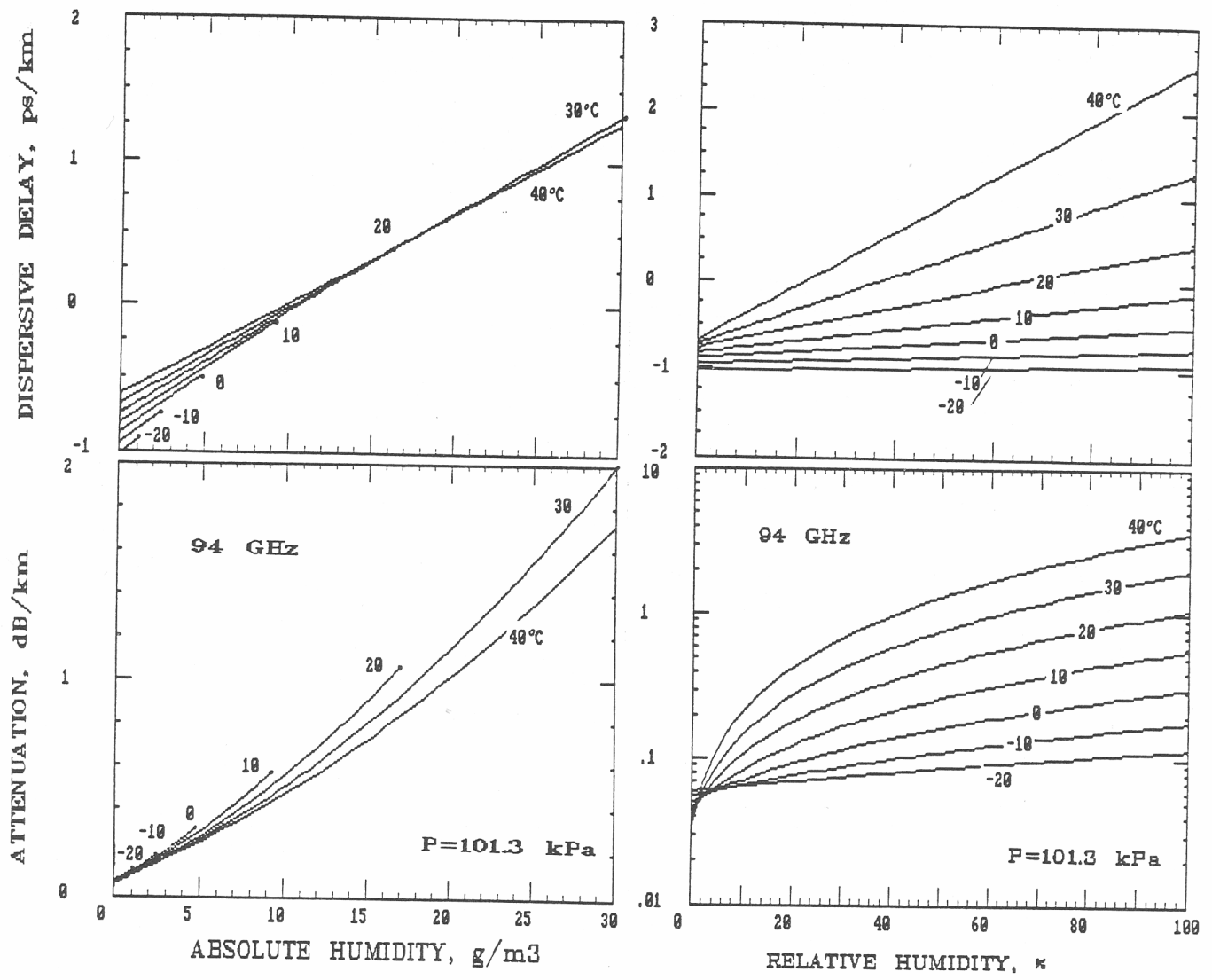


Figure 12. Absolute (ν) and relative (RH) humidity dependence of attenuation α and delay β at $f = 94$ GHz for various sea level conditions ($P = 101.3$ kPa and $T = -20$ to 40°C).

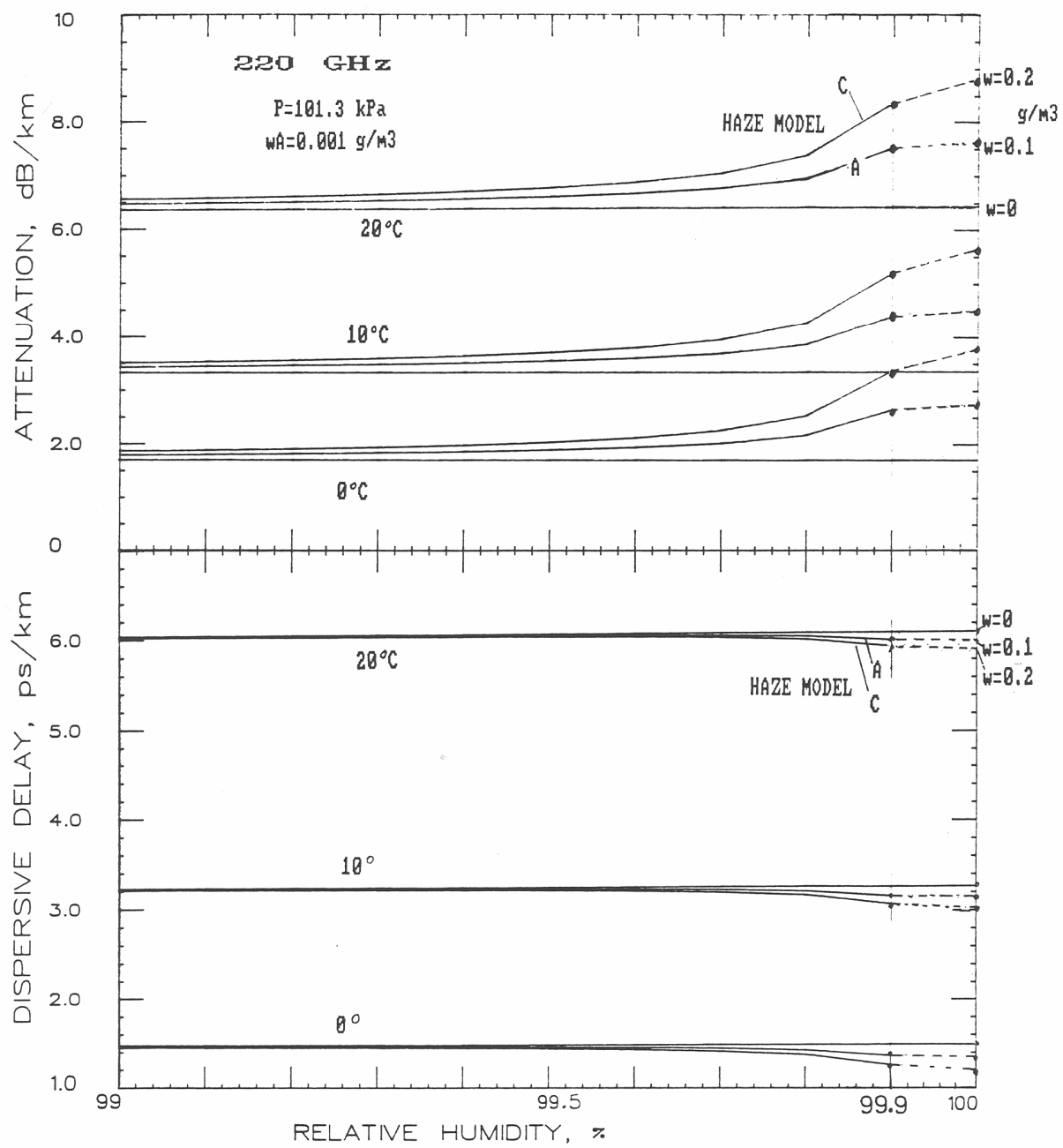


Figure 13. Two haze cases (A: 1 mg/m^3 and C: 1 mg/m^3) for prefog ($\text{RH} = 99-99.9\%$) and fog ($w=0.1$ and 0.2 g/m^3) conditions at three temperatures ($0, 10, 20^\circ\text{C}$) displaying the associated attenuation α and delay β rates at $f = 220 \text{ GHz}$.

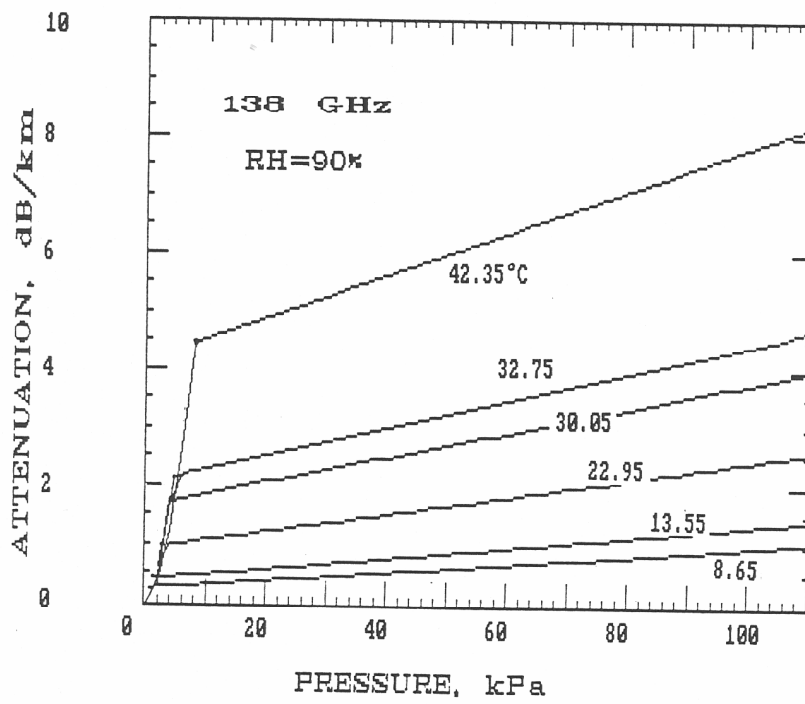
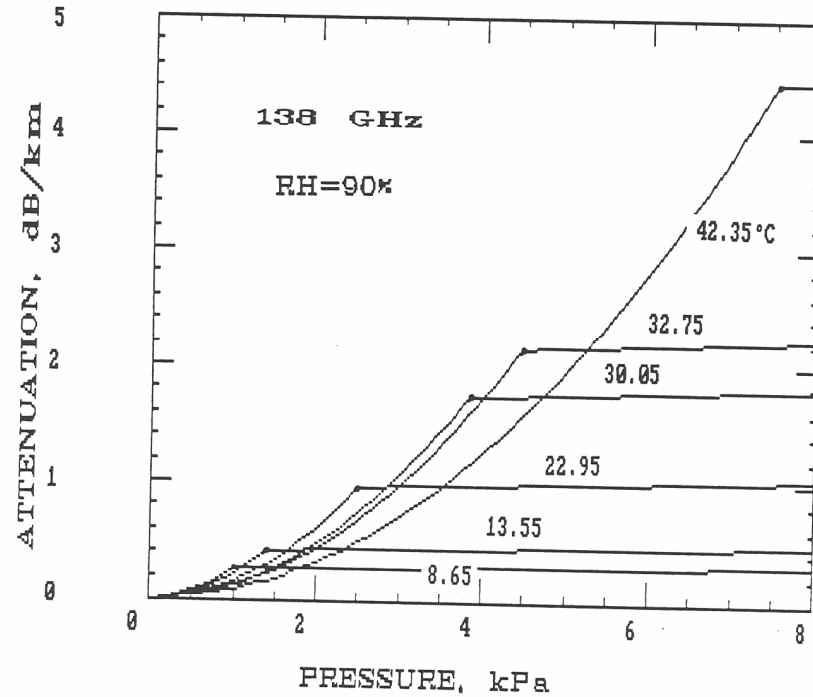


Figure 14. Pressure profiles at $f = 138$ GHz simulating the laboratory attenuation measurements presented in Section 2.3.

coefficients a_5 (see page 66) were adapted for MPM, and Table 5 demonstrates the degree of agreement.

4.1 Laboratory Measurements

The results on moist air attenuation at 138 GHz [i.e., (5), (8)] provided clues to a formulation of an empirical MPM water vapor continuum. Data from other researchers were evaluated to check if the assumptions of (10) held up at different frequencies. Water vapor attenuation at frequencies between 330 and 430 GHz is compared with MPM predictions in Figure 15. The data were available in graphic form and had to be digitized by us. Considering the many difficulties that plague absolute calibrations, a comparison of model vs. experiment is encouraging. No anomalous absorption features have been uncovered.

Two laboratory studies of the 183-GHz water vapor line have been reported by a French group [11], [17]. We adapted the width results [11] for the line table of MPM. A detailed analysis of temperature-dependent wing data [17] is given in Table 6. Equation (5) was applied to reduce both experimental and MPM data for an intercomparison. At +1 GHz from the line center, the attenuation rate for pure water-vapor shows a discrepancy of 21 percent. The origin of such disagreement has to be attributed to the 183-GHz line broadening formulation but not to the rather small contribution from the continuum.

4.2 Field Measurements

Ultimately, it is up to field experiments to garner realistic evidence in support of model predictions. When conducted with care at different locations under a variety of natural conditions, such experiments prove to be quite costly.

Data from ITS field studies on the propagation of millimeter waves were evaluated for water-vapor attenuation rates at 96.1 GHz [18], [19]. Clear air data and MPM predictions are in close agreement, allowing for the temperature dependence, as demonstrated in Figure 16. The mission of these experiments was to establish a data base for 11.4 to 96.1 GHz propagation in a humid climate (Huntsville, AL, April-August 1986). A similar comparison was not so favorable for a set of data displayed in Figure 17. The results were obtained over a 1.5 km line-of-sight path in the Soviet Union at subfreezing

Table 5. Measured (EXP) and Predicted (MPM) Dispersion in Dry Air at 300 K
 (Interference Coefficients from Rosenkranz [10])

| Nearby Line | Frequency GHz | Dispersion N'(f) | | Frequency GHz | Dispersion N'(f) | |
|-------------|------------------|------------------|---------------------|------------------|------------------|---------------------|
| | | EXP ppm | MPM p = 53.3 kPa | | EXP ppm | MPM p = 80.0 kPa |
| 25- | 53.588 | 0.30 | 0.300 | 53.585 | 0.43 | 0.439 |
| 23- | 54.123 | 0.35 | 0.338 | 54.119 | 0.50 | 0.490 |
| 19- | 55.214 | 0.40 | 0.407 | 55.210 | 0.58 | 0.576 |
| 17- | 55.776 | 0.42 | 0.421 | 55.772 | 0.60 | 0.589 |
| 15- | 56.356 | 0.41 | 0.398 | 56.352 | 0.59 | 0.565 |
| 13- | 56.960 | 0.38 | 0.350 | 56.956 | 0.45 | 0.502 |
| 3+ | 58.439 | 0.19 | 0.174 | 58.435 | 0.26 | 0.253 |
| 7- | 59.156 | 0.08 | 0.076 | 59.152 | 0.12 | 0.110 |
| 5+ | 59.583 | 0.03 | 0.027 | 59.579 | 0.03 | 0.032 |
| 5- | 60.296 | -0.075 | -0.084 | 60.292 | -0.11 | -0.134 |
| 7+ | 60.425 | -0.135 | -0.122 | 60.421 | -0.17 | -0.170 |
| 9+ | 61.141 | -0.275 | -0.252 | 61.136 | -0.383 | -0.361 |
| 11+ | 61.790 | -0.335 | -0.342 | 61.785 | -0.510 | -0.522 |
| 13+ | 62.400 | -0.480 | -0.475 | 62.396 | -0.685 | -0.679 |
| 3- | 62.475 | -0.510 | -0.495 | 62.471 | -0.720 | -0.705 |
| 15+ | 62.987 | -0.590 | -0.578 | 62.983 | -0.80 | -0.800 |
| 17+ | 63.558 | -0.610 | -0.589 | 63.554 | -0.841 | -0.831 |

Table 6. Comparison between MPM-Predicted and Experimental Attenuation for Water Vapor (e) and Moist Air ($P = e_1 + p$) in the Wing Region of the H₂O Line Centered at $\nu_0 = 183.310$ GHz

| f, GHz | $\nu_0 + 3.0$ | $\nu_0 + 1.0$ | $\nu_0 + 0.4$ | MPM - PREDICTIONS | | | | | |
|---------------------|-----------------------|---------------|---------------|----------------------|-------|-------|----------------------|-------|-------------------|
| | | | | 1.059kPa (7.94 torr) | | | 0.529kPa (3.97 torr) | | |
| e_1 | 1.766kPa (13.25 torr) | | | Lines | Cont. | Total | Lines | Cont. | Total |
| | T K | | | 3.66 | 0.53 | 4.19 | 11.35 | 0.19 | 11.54 |
| α , dB/km | 310 | 3.66 | 0.53 | 4.19 | 12.90 | 0.25 | 13.15 | 17.37 | 0.05 |
| | 300 | 4.17 | 0.70 | 4.87 | 14.17 | 0.33 | 15.05 | 19.73 | 0.06 |
| | 290 | 4.76 | 0.95 | 5.71 | | | | 22.49 | 0.08 |
| P | 100kPa (750 torr) | | | 21.52 | 1.83 | 23.52 | 21.39 | 0.95 | 22.52 |
| α , dB/km | 310 | 23.59 | 2.07 | 25.86 | 23.10 | 1.06 | 24.35 | 11.66 | 0.43 |
| | 300 | 25.92 | 2.40 | 28.53 | 25.00 | 1.19 | 26.41 | 12.57 | 0.47 |
| | 290 | | | | | | | 13.58 | 0.51 |
| | | | | 100kPa (750 torr) | | | 100kPa (750 torr) | | 100kPa (750 torr) |

DATA REDUCTION: MPM-vs-EXPERIMENT

| | <u>MPM</u> | <u>EXP*</u> | <u>X/M</u> <u>%</u> | <u>MPM</u> | <u>EXP*</u> | <u>X/M</u> <u>%</u> | <u>MPM</u> | <u>EXP*</u> | <u>X/M</u> <u>%</u> |
|-------|------------|-------------|------------------------|------------|-------------|------------------------|------------|-------------|------------------------|
| k_s | 300 | 1.56 | 1.67 | 7.1 | 11.72 | 14.2 | 21.2 | 70.56 | 75.3 |
| x_s | - | 4.56 | 4.1 | -10.1 | 3.99 | 3.9 | -2.3 | 3.88 | 3.5 |
| k_f | 300 | 0.121 | 0.136† | 12.4 | 0.107 | - | | N.A. | 6.7 |
| x_f | - | 2.48 | 2.7 | 8.9 | 1.96 | - | | N.A. | -9.8 |
| m | 300 | 0.0776 | 0.0814 | 4.9 | 0.0913 | - | | N.A. | |

*Reference [17],

†N₂-result reduced by 0.907.

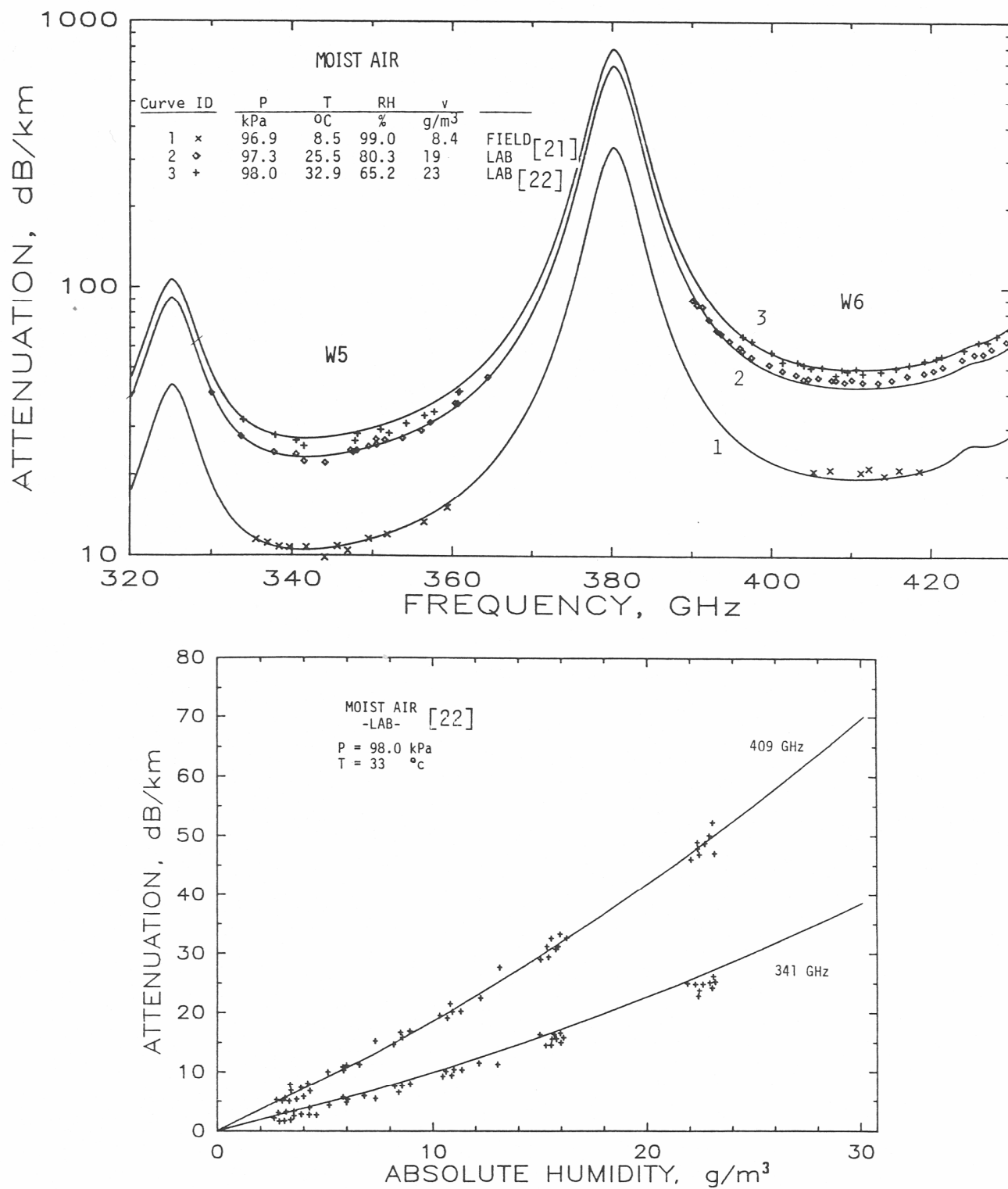


Figure 15. Moist air attenuation $\alpha(f)$ across the atmospheric window ranges W5 and W6 (320 to 430 GHz) at temperatures 8.5, 25.5, and 32.9°C: data points [21], [22]; solid lines, MPM.

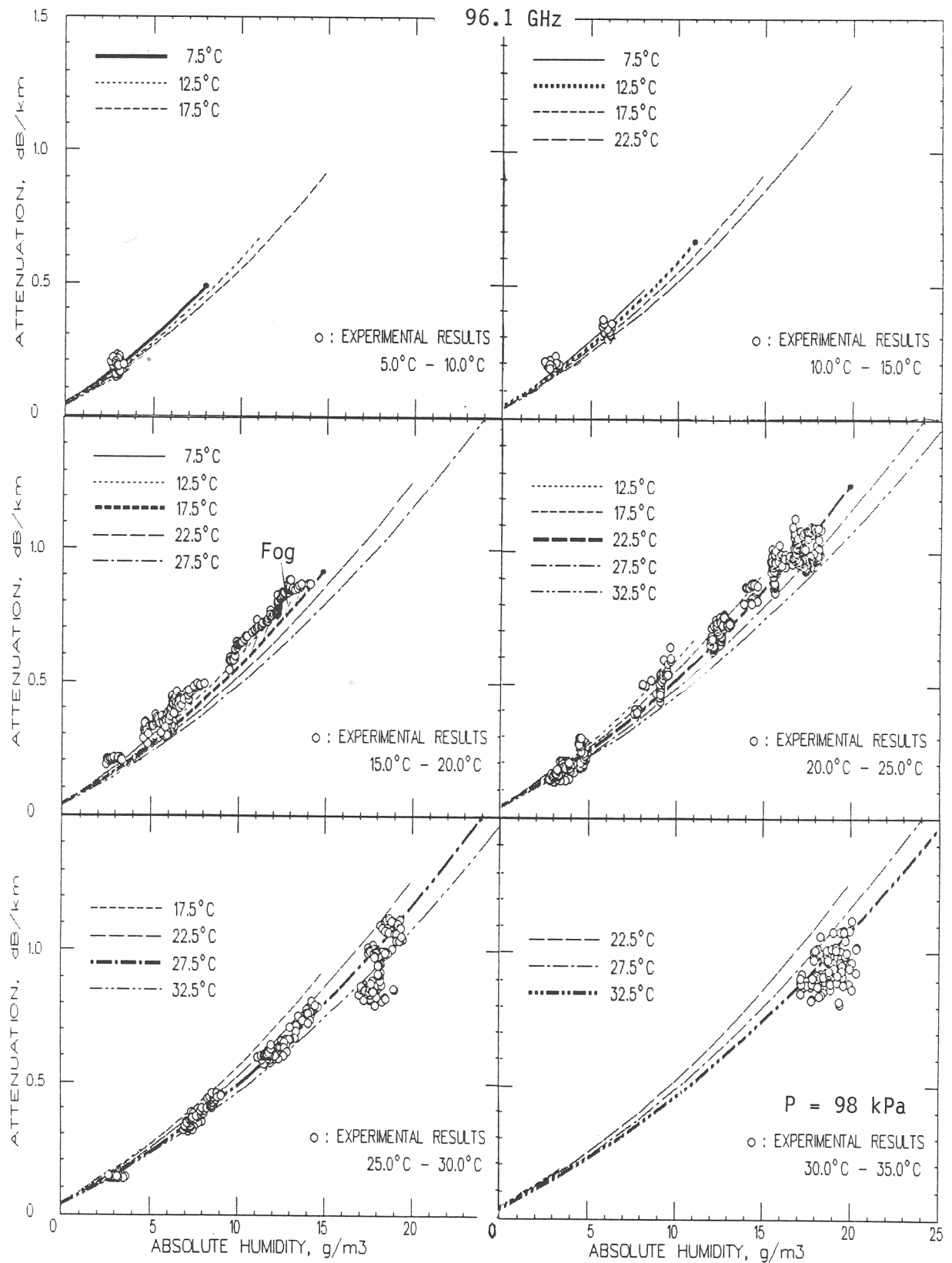


Figure 16. Moist air attenuation $\alpha(v)$ measured at 96.1 GHz over a 21.4 km line-of-sight path located in Huntsville, AL ($h = 0.3$ km) for six temperature groups between 2.5 and 37.5°C [19] data points are 5-min averages for 4.5 days (5/4-6, 8/15-16/1986); solid lines, MPM.

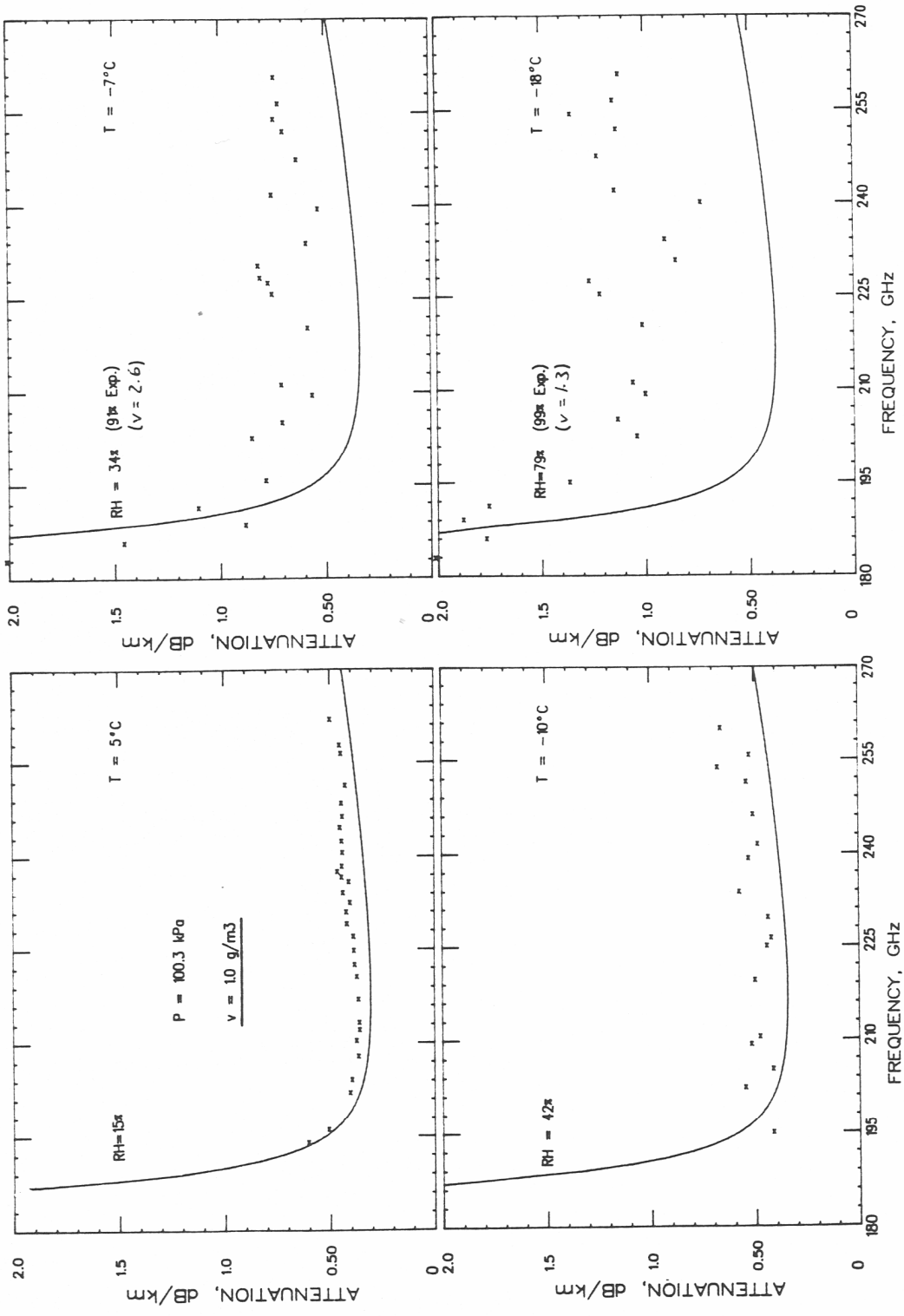


Figure 17. Water vapor attenuation rates $\alpha(v)$ across the atmospheric window range W4 at four temperatures, 5, -7, -10, and -18°C : data points [20]; solid lines [20].

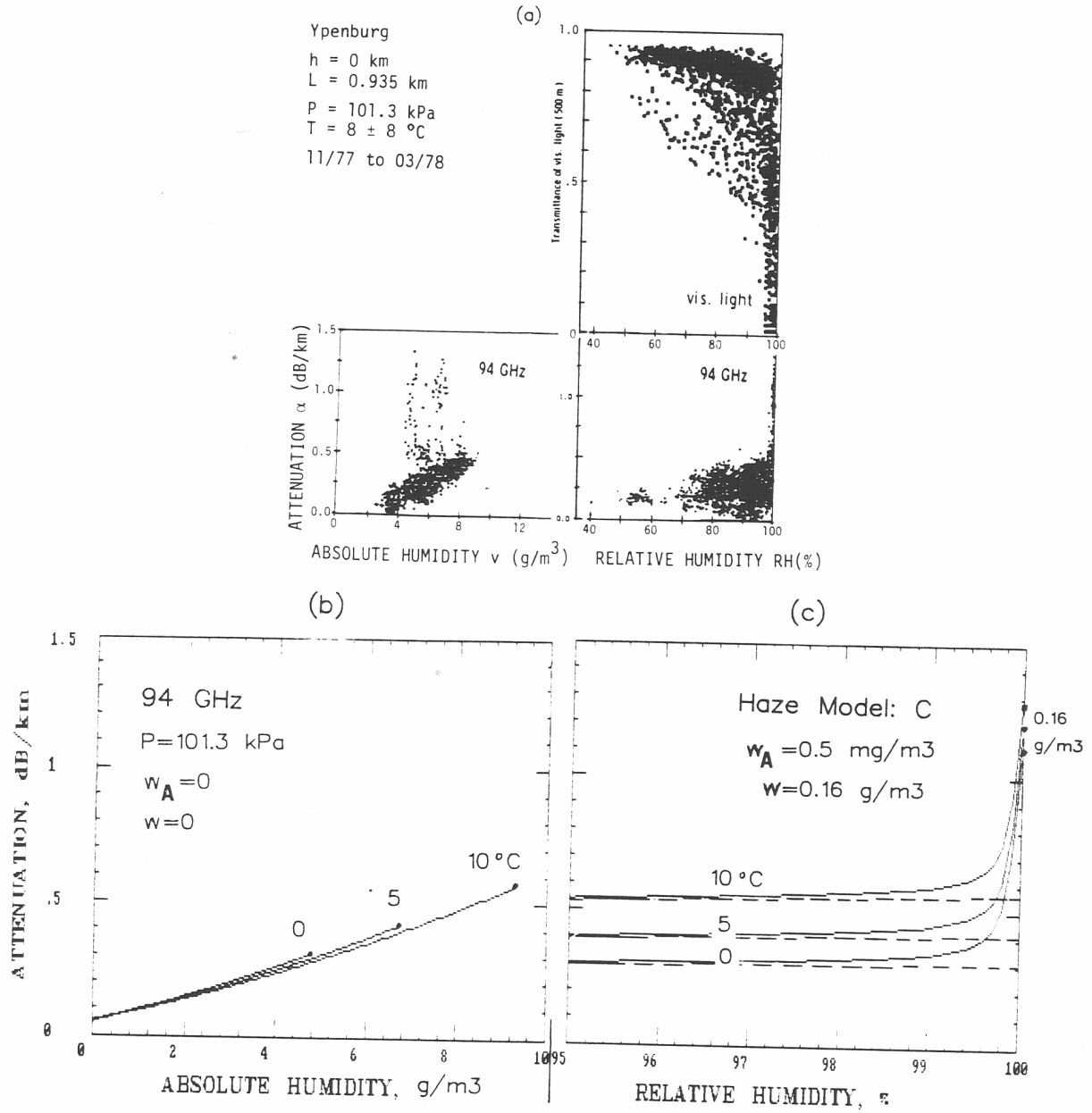


Figure 18. Terrestrial path attenuation at 94 GHz and $0.65 \mu\text{m}$ (visible light) under nonprecipitating conditions as a function of absolute (v) and relative (RH) humidity [3]: (a) data points, 5-min averages taken every 30 min during a period of 4 months [23]; (b) MPM simulation of (a) for absolute humidity; (c) MPM simulation of (a) over the range, RH = 95 to 100%, including haze model C.

temperatures for frequencies between 192 and 260 GHz [20]. Experimental uncertainties are not discussed, the extreme environmental conditions may have played a role. On the other hand, 335 - 420 GHz field data (included in Figure 15), that were reported by another group from the Soviet Union [21], [22] agree remarkably well with MPM predictions.

Attenuation data at 94 GHz have been recorded in a coastal region of the Netherlands [23]. Data, when presented in Figure 18 versus absolute humidity v , display significant random excess attenuation over MPM predictions. The same data plotted versus RH places all excess attenuation at $RH > 98\%$. Haze and fog conditions probably were present as evident from optical transmission data. The highest excess of 0.8 dB/km requires $w \approx 0.16 \text{ g/m}^3$, a value typical for heavy fog.

Figure 19 presents atmospheric noise temperatures measured against zenith at two different sites simultaneously at 10, 33, and 90 GHz [24]. Predictions with the MPM radio path program reproduce the frequency correlations quite correctly, which tends to confirm the f^2 assumption made for H_2O continuum absorption (10). In addition, model data set a limit for total precipitable water vapor $V[\text{mm}]$ carried by the air mass. Noise exceeding this limit probably originates from suspended droplets. Data trends stemming from differences in the f -dependence of moist air and SWD absorption support such assumption.

5. CONCLUSIONS

Radio properties of the atmosphere are both a barrier and a boon to applications in the 10-1000 GHz spectral range. The first part of this report gave a somewhat detailed description of a laboratory experiment that had to apply latest advances in digital electronics and cryogenic detection to derive at 138 GHz two attenuation coefficients, k_s and k_f (8). At first sight, these two quantities describe the attenuation rate of moist air over a rather inconspicuous range from 0.1 to 10 dB/km; however, a more detailed analysis revealed the k -formulation provides conclusive evidence on temperature and pressure dependence of the water vapor continuum. Attaching an f^2 dependence to the 138-GHz results turned a frequency limited ($< 1 \text{ THz}$) propagation model into a useful tool capable of operating in frequency, humidity, and pressure domains of the atmosphere.